Global Journal of Pure and Applied Mathematics.
ISSN 0973-1768 Volume 10, Number 5 (2014), pp. 697-705

http://www.ripublication.com

A Lattice Boltzmann Simulation for Modeling the Non-Newtonian Blood Flow

Somchai Sriyab

Department of Mathematics, Chiang Mai University, Chiang Mai, Thailand, 50200
Tel:+66 053-943327#116, Fax: +66 053-892280, e-mail:somchai.sriyab@gmail.com.

ABSTRACT

The Lattice Boltzmann method (LBM) is used to simulate the flow of non-Newtonian blood, considering that viscosity is a function of the velocity gradient in the Casson model. Analytical solutions have been derived to validate the Lattice Boltzmann scheme. The agreement between the velocity profile of LBM for non-Newtonian blood and the profile values obtained in the analytic solutions is excellent. Therefore, LBM can be used as a tool to study the blood rheology in the non-Newtonian model. The numerical results of LBM are found to be corresponding to the experimental result that blood behaves in a non-Newtonian manner at low shear rates and becomes Newtonian at high shear rates.

Keywords: non-Newtonian, Casson's rheology model, Lattice Boltzmann method (LBM)

1. Introduction

Blood is a marvelous fluid that nurtures life; it contains many enzymes, hormones, and oxygen. The study of the important functions of blood can be left to hematologists, biochemists, and pathological chemists. However, the most important information as far as biomechanics is concerned is the constitutive equation [1]. The Newtonian constitutive equation is used to describe the behavior of blood flow in larger diameter arteries, while the non-Newtonian equation is used for smaller diameter arteries [2]-[4]. In this paper, we study the non-Newtonian model, namely, the Casson model, which is widely used to investigate blood flow in smaller arteries. The study in [5] suggested that the Casson model is appropriate to study the flow in smaller arteries. Merrill and coworkers observed that the Casson model can predict satisfactorily the blood flow behavior in tubes with diameters in the range of 130–1000 μm [6]. Blair and Copley showed that the Casson model is an adequate model

for the study of simple shear behavior of blood flow in small arteries ([7], [8]). Charm and Kurland showed that the Casson model could be applied to human blood at wide ranges of hematocrit and shear rates [9]. The Lattice Boltzmann method (LBM) is a novel numerical approach that has recently been adapted to blood rheology and particle interaction in blood flow. In this method, a discretized BGK form of LBM for the fluid particle distribution function is solved on a uniform lattice. In our work, LBM has been developed for the Casson model, and the numerical results are compared with the results of the analytical solution for a two-dimensional blood flow between parallel plates, where the governing equations can be solved analytically.

2. Mathematical analysis.

Blood behaves as a non-Newtonian fluid when it flows in the region of small vessels [10]-[15]. The Casson rheology model is defined as follows:

$$\sqrt{\sigma} = \sqrt{\eta_c \dot{\gamma}} + \sqrt{\sigma_y} \tag{1}$$

where σ is the shear stress, η_c is the Casson viscosity, σ_y is the yield stress and $\dot{\gamma}$ is the shear rate. Since the apparent viscosity (μ) is defined as $\mu(\dot{\gamma}) = \frac{\sigma}{\dot{\gamma}}$, we obtain

$$\mu(\dot{\gamma}) = \frac{(\sqrt{\eta_c \dot{\gamma}} + \sqrt{\sigma_y})^2}{\dot{\gamma}} \tag{2}$$

In order to calculate the local relaxation time (τ), the following equation is used

$$\tau = 3\mu + \frac{1}{2} \tag{3}$$

The relation between viscosity (μ) and shear rate $(\dot{\gamma})$ is determined, as shown in Figure 1, by using the parameter from Perktold and coworkers ([16], [17]). The viscosity decreases rapidly when the shear rate increases from 0 to 10 second^{-1}. Thereafter, it decreases very slightly with the increase in the shear rate. As a result, blood behaves in a non-Newtonian manner when the shear rate is below 10 second^{-1}.

As for the case of fluid flow between two parallel plates, the conservation of momentum leads to the following equation:

$$\sigma = \mu \frac{\partial U}{\partial y} = y \frac{\partial P}{\partial x} \tag{4}$$

where U is the velocity flow in x direction and P is the pressure. When the shear rate is equal to yield stress, the equation is obtained as follows:

$$y_c = \sigma_y \left(\frac{\partial P}{\partial x}\right)^{-1} \tag{5}$$

Upon simplifying equation (1), we get the following:

$$\dot{\gamma} = \frac{\sigma - 2\sqrt{\sigma \sigma_y} + \sigma_y}{\eta_c} \tag{6}$$

Since we consider the blood flow in only the y direction, the stress rate $(\dot{\gamma})$ is computed by using the first order finite difference approximation:

$$\frac{U(y+h)-U(y)}{h}=\frac{\sigma-2\sqrt{\sigma\sigma_y}+\sigma_y}{\eta_c} \tag{7}$$

If $h\to 0$, the equation (7) becomes the following:

$$U'(y)=\frac{\sigma-2\sqrt{\sigma\sigma_y}+\sigma_y}{\eta_c} \tag{8}$$

Upon substituting equations (4) and (5) in equation (8), we get the following:

$$U'(y)=\frac{y\frac{\partial P}{\partial x}-2\sqrt{yy_c}\left|\frac{\partial P}{\partial x}\right|+y_c\frac{\partial P}{\partial x}}{\eta_c} \tag{9}$$

By integrating equation (9), the analytic solution of the Casson's model is obtained:

$$U(y)=\frac{1}{\eta_c}\left(\frac{y^2-L^2}{2}\right)\frac{\partial P}{\partial x}-\frac{4}{3}\sqrt{y_c}\left|\frac{\partial P}{\partial x}\right|\left(\sqrt{|y|^3}-\sqrt{L^3}\right)+y_c\frac{\partial P}{\partial x}(|y|-L) \tag{10}$$

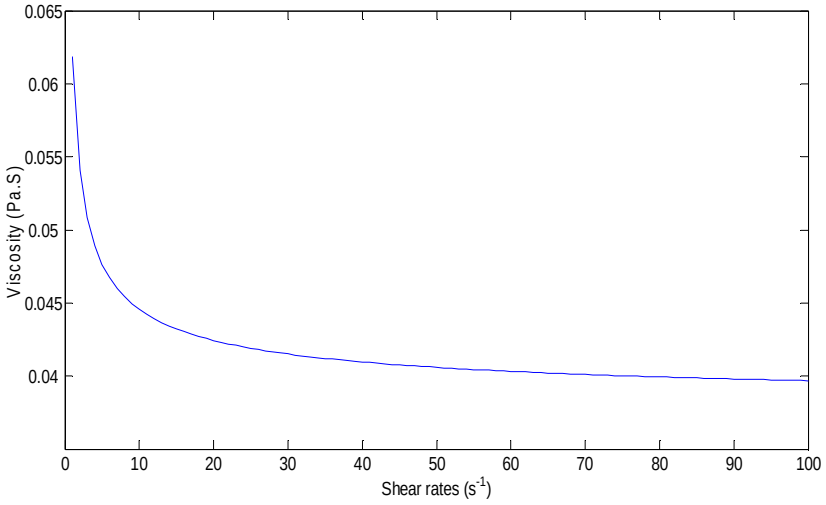

Figure1. The relation between Shear rate $(\dot{\gamma})$ and viscosity (μ)

3. The Lattice Boltzmann method.

A new numerical technique for simulating complex flow and transport phenomena, LBM provides an alternative approach where direct solution of the Navier-Stokes equations is not practical. The traditional computational methods in fluid dynamics (finite element method, finite difference method, and finite volume method) solve macroscopic fluid dynamics equations, while LBM solves a problem at a microscopic level in order to recover the particle density and the velocity from macroscopic properties ([18]). LBM consists of simple arithmetic calculations, which are easy to program. The space in LBM is divided into a regular Cartesian lattice grid as a consequence of the symmetry of the discrete-velocity set. Each lattice point has an assigned set of velocity vectors with specified magnitudes and directions. The total

velocity and the total particle density are defined by specifying the number of particles associated with each of the velocity vectors. The macroscopic particle distribution function is unknown in that it evolves at each time step through a two-step procedure: convection and collision. The first step, convection, simply advances the particle from one lattice site to another lattice site along the directions of motion according to their velocities. The second step, collision, is to imitate various interactions among the particles.

The Lattice Boltzmann equation can be viewed as a discrete form of the Boltzmann equation. LBM can be derived directly from the simplified Boltzmann Bhatnagar–Gross-Krook (BGK) equation ([18]–[19]). The discrete form of the Lattice Boltzmann equation is as follows:

$$f_\alpha(\vec{r}+\Delta t\vec{c}_\alpha, t+\Delta t) = f_\alpha(\vec{r},t) + \Omega_\alpha(\vec{r},t) \tag{11}$$

where f_α is the distribution function at space $\vec{r}$ and time t .The particle distribution travel to the next lattice node in a time step Δt and the discrete velocity $\vec{c}_\alpha$ .The collision operator Ω_α differs according to the model details. In the lattice BGK (LBGK) that we use, the particles distribution after propagation is relaxed toward the equilibrium distribution $f_i^{eq}(\vec{r},t)$ according to

$$\Omega_\alpha(\vec{r},t) = -\frac{1}{\tau}(f_\alpha(\vec{r},t) - f_\alpha{}^{eq}(\vec{r},t)) \tag{12}$$

The relaxation parameter τ determines the kinematic viscosity μ of the simulated flow as follows:

$$\mu = (2\tau - 1)/6 \tag{13}$$

The equilibrium distribution f^{eq} is defined for two dimensional as follows:

$$f_\alpha{}^{eq} = \omega_\alpha \rho(1 + \frac{3c_\alpha \cdot \vec{u}}{c^2} + \frac{9(c_\alpha \cdot \vec{u})^2}{2c^4} - \frac{3u^2}{2c^2}) \tag{14}$$

The weight constant and the lattice velocities are the following:

$$\omega_\alpha = \begin{cases} 4/9 & \alpha = 0 \\ 1/9 & \alpha = 1,2,3,4 \\ 1/36 & \alpha = 5,6,7,8 \end{cases} \tag{15}$$

$$c_\alpha = \begin{cases} (0,0) & \alpha = 0 \\ c(\cos\theta_\alpha, \sin\theta_\alpha), \ \theta_\alpha = (\alpha\text{-}1)\pi/2 & \alpha = 1,2,3,4 \\ \sqrt{2}c(\cos\theta_\alpha, \sin\theta_\alpha), \ \theta_\alpha = (\alpha\text{-}5)\pi/2 + \pi/4 & \alpha = 1,2 \end{cases} \tag{16}$$

The density (ρ) and the flow velocity (u) can be calculate from

$$\rho = \sum_{\alpha=0}^{8} f_\alpha \tag{17}$$

$$\rho u = \sum_{\alpha=0}^{8} C_\alpha f_\alpha \tag{18}$$

4. Numerical results and discussion

The objectives of our study were that we discuss the numerical results from the investigation of non-Newtonian and Newtonian blood flow by using LBM and compare the numerical results with those from the analytical solution. To implement LBM, we used D2Q9 for the Casson's model. The bounce back boundary condition is used for solid walls, while the inlet and outlet boundaries are the periodic boundary conditions. The viscosity (μ) and the relaxation time (τ) are constant in the case of the Newtonian fluid, while the viscosity is a function of the velocity gradient in the case of the non-Newtonian fluid. All the parameters in the simulation are defined in a dimensionless lattice unit.

$$\mathrm{Re} = \frac{\rho \frac{\partial P}{\partial x} (2L)^3}{12\mu} \tag{19}$$

From equation (19), we obtain the indication that the Reynolds number (Re) increases with the decrease in the blood viscosity (μ). Figure 1 demonstrates that blood viscosity (μ) decreases with an increase in the shear rate $(\dot{\gamma})$. From equation (19) and Figure 1, we can conclude that the Reynolds number (Re) increases with an increase in the shear rate $(\dot{\gamma})$. The normalized velocity with the channel width for different Reynolds numbers (Re) and Newtonian flow is shown in Figure 2. Here, we notice that when the Reynolds number (Re) increases, the blood velocity profile approaches a parabolic shape that is the same as the velocity profile of the Newtonian fluid. These numerical results are in accordance with the experimental observation ([2]). From the experimental results, it can be seen that the blood is almost non-Newtonian in behavior at low shear rates, but it is Newtonian in behavior at high shear rates. One should note that the dimensionless velocity profiles of the Newtonian blood flow are identical with the different Reynolds numbers (Re). In order to validate the Lattice Boltzmann results, the plots of the numerical and analytic velocity profiles for the different Reynolds numbers are sketched in Figures 3–7. It can be observed that the numerical velocity profiles are in excellent agreement with the analytic velocity profiles. Figure 3 and Figure 4 demonstrate that the velocity profile increases slightly when the channel width increases from 0 to 50, and then it decreases slightly when the channel width increases from 50 to 100. Figures 5–7 show that the velocity profile increases marginally when the channel width increases from 0 to 50, and then it decreases marginally when the channel width increases from 50 to 100.

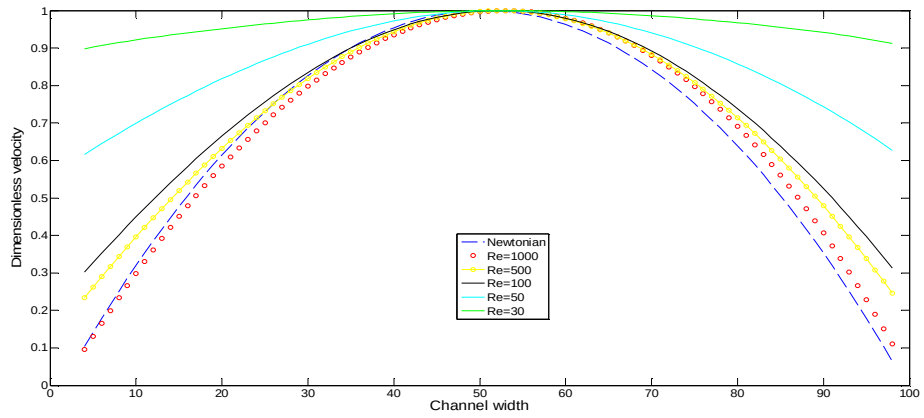

Figure2. The velocity profiles with the channel width for different Reynolds number (Re) **and Newtonian**

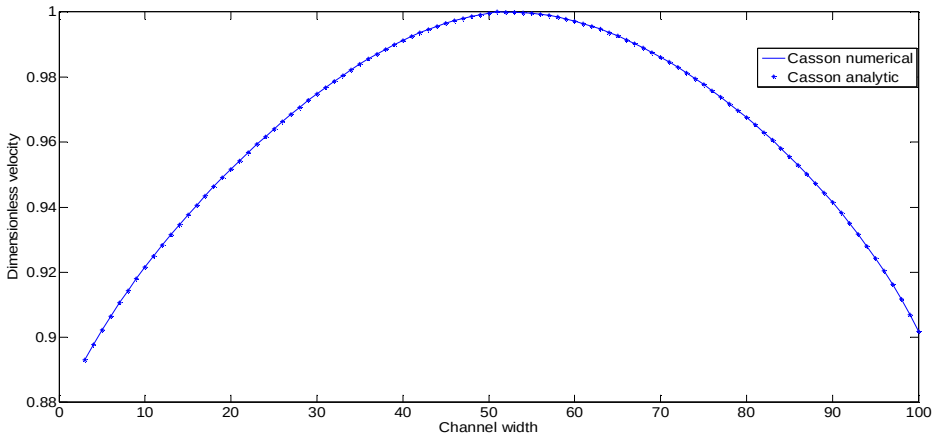

Figure3. The velocity profile of non-Newtonian blood flow and the exact solution for Re = 30

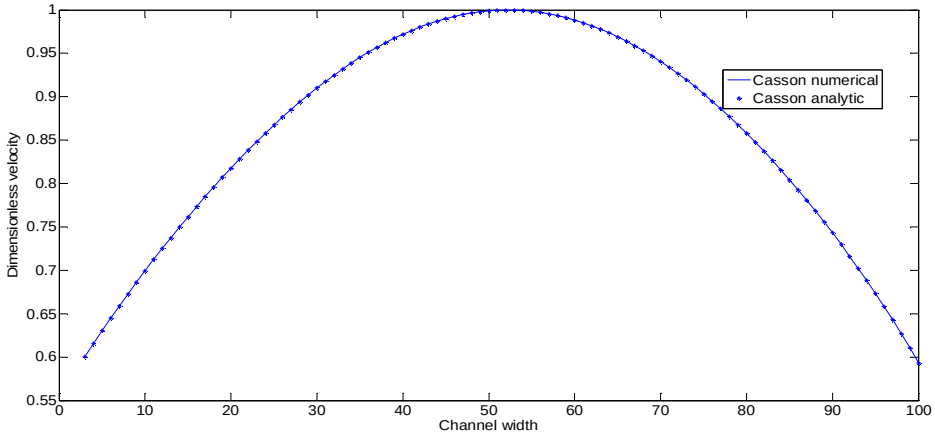

Figure4. The velocity profile of non-Newtonian blood flow and the exact solution for Re = 50

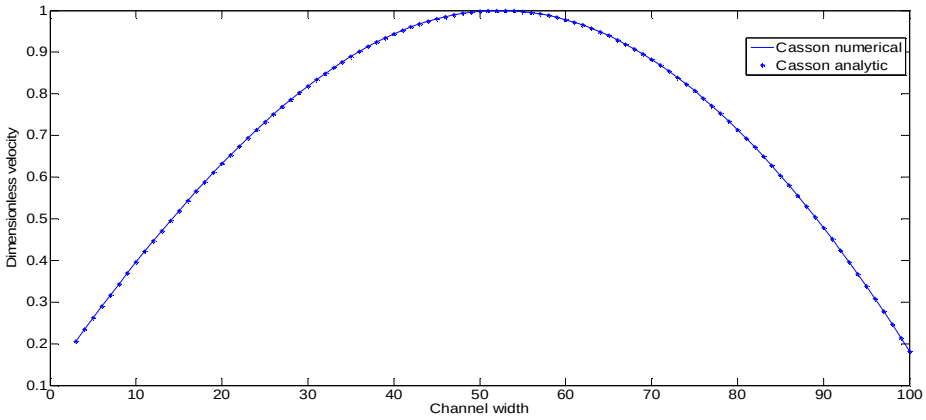

Figure5. The velocity profile of non-Newtonian blood flow and the exact solution for $\mathrm{Re}=100$

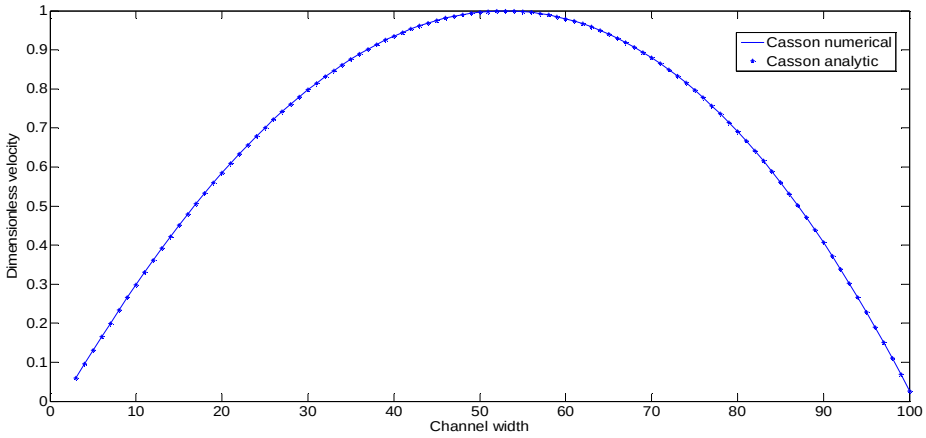

Figure6. The velocity profile of non-Newtonian blood flow and the exact solution for $\mathrm{Re}=500$

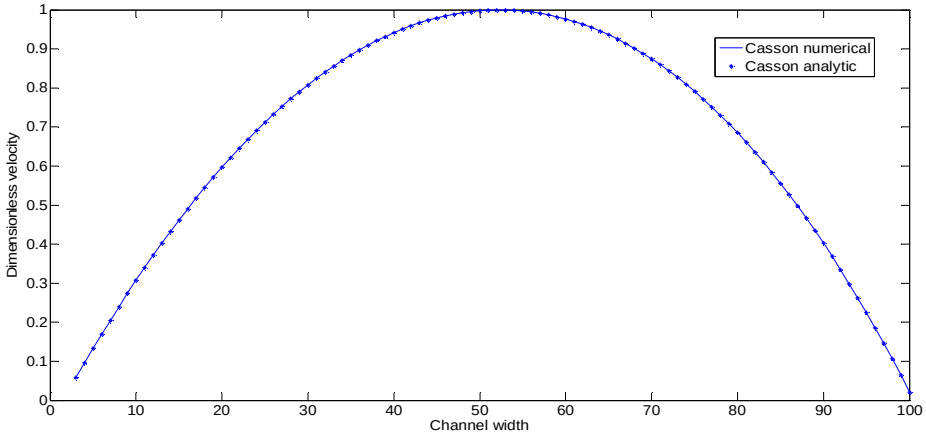

Figure7. The velocity profile of non-Newtonian blood flow and the exact solution for $\mathrm{Re}=1,000$

4. Conclusion

A D2Q9 Lattice Boltzmann method was developed to investigate blood rheology in the non-Newtonian flow of the Casson model and in Newtonian fluids. The velocity profile of LBM for non-Newtonian flow was found to be in excellent agreement with the profiles of the analytical solutions. These results demonstrate the capacity of LBM when it comes to non-Newtonian blood flow simulations. Additionally, we found that blood exhibits the properties of a non-Newtonian fluid at low shear rates, but it behaves like a Newtonian fluid at high shear rates.

5. Acknowledgment

This research work was supported by the Department of Mathematics, Faculty of Science, Chiang Mai University, Thailand.

References

[1] Fung, Y.C., 1993, Biomechanics, Mechanical Properties of Living Tissues, 2nd ed., Springer, New York, USA, Chap3-4.

[2] Rathod, V. P., and S.Tanveer., 2009, " Pulsatile flow of couple stress fluid through a porous medium with periodic body acceleration and magnetic field, " Bulletin of the Mathematical Science. pp.32245-259.

[3] Mazumdar, J.N., 1992, Biofluid Mechanics, World Scientific, Singapore, Chap. 2-4.

[4] Fournier, R.L., 2007, Basic Transport Phenomena in Biomedical Engineering, Taylor& Francis, London, chap 4.

[5] Casson N., 1959, Rheology of Disperse System, Pergamon Press, London, UK, chap. 2.

[6] Merrill, E.W., Benis, A.M., Gililand, E.R., Sherwood, T.K., and Salzmann, E.W., 1965, " Pressure flow relations of human blood in hollow fibers at low flow rate, " Journal of Applied Physiology, pp.20954-967.

[7] Blair, G.W.S., 1959, " An equation for the flow of blood, plasma and serum through glass capillaries, Nature, " 183, pp. 613-614.

[8] Copley, A.L., 1959, Flow Properties of Blood and Other Biological Systems, Pergamon Press, Oxford, UK, chap. 3.

[9] Charm, S., and Kurland, G., 1965, " Viscometry of human blood for shear rates of 0-100, 000 sec^{-1}, " Nature, 206, pp. 617-618.

[10] Malek, A.M., Alper, S.L., and Izumo, S., 1999, " Hemodynamics shear stress and its role in atherosclerosis, " J. Am. Med. Assoc. 282, pp. 2035-2042.

[11] Asakura, T. and Karino, T., 1990, " Flow patterns and spatial distribution of atherosclerotic lesion in human coronary arteries, " Circ. Res. 66, pp.1045-1066.

[12] Gnasso, A. C., Irace, C., Carallo, M. S., Franceschi, D., Motti, C., Mattioli, P. L., and Pujia, A., 1997, " In vivo association between low wall shear stress and plaque in subjects with asymmetrical carotid atherosclerosis, " Stroke. 28, pp 993-998.

[13] Ku, D. N., Giddens, D. P. C., Zarins, K. and Glagow, S., 1985, " Pulsatile flow and atherosclerosis in the human carotid bifurcation: Positive correlation between plaque location and low oscillating shear stress, "Arteriosclerosis (Dallas). 5, pp. 293-302.

[14] Chappell, D., Varner, C. S. E., R. M., Medford, R. M., and Alexander, R. W., 1998, " Oscillatory shear stimulates adhesion molecule expression in cultured human endothelium ", Cir. Res. 82, pp. 532-539.

[15] Artoli, A.M., Hoekstra, A. G., and Sloot, P. M. A., 2006, " Mesoscopic simulations of systolic flow in the human abdominal aorta, "J. Biomech. 39, pp. 873-884.

[16] Liboff, R. L., 1990, Kinetic Theory, Prentice Hall, Englwood Cliffs, NJ, USA, chap.3.

[17] Zhaoli, G., Zhao, T. S. and Yong, S., 2005, " A Lattice Boltzmann algorithm for electroosmotic flow in microfluid devices, " J. Chem. Phys. 122, pp.144907.

[18]Harris, S., 1971, An Introduction to the theory of the Boltzmann equation, Holt Rinechart and Winston, New York, USA.

[19] Somchai, S., Jiraporn Y., Waipot, N., Paisan, K., Charin, M., Narin, N., Yongwimon, L., Chartchai, K., and Wanapong T., 2009, " Mesoscale Modeling Technique for dynamics oscillation of min proteins: Pattern formation analysis with Lattice Boltzmann method, " Comp. Bio.Med. 39, pp. 412-424.

.